

Thermal stability of a quantum rotation sensor

Ehsan Arabahmadi^{1,*}, Daniel Schumayer^{1,†}, Mark Edwards^{2,‡}, Ben Eller³, and David A. W. Hutchinson^{1,2,4,§}

¹*Dodd-Walls Centre for Photonic and Quantum Technologies, Department of Physics, University of Otago, Dunedin 9016, New Zealand*

²*Department of Physics, Georgia Southern University, Statesboro, Georgia 30460-8031, USA*

³*Chemical Physics Program, University of Maryland, College Park, Maryland 20742, USA*

⁴*Centre for Quantum Technologies, National University of Singapore, Singapore 117543*



(Received 6 July 2021; accepted 7 September 2021; published 28 September 2021)

We investigate the thermal instability of a Bose-Einstein condensate stirred by a rotating barrier in a ring-shaped trap. One would expect the critical angular speed to decrease with increasing temperature due to depletion of the condensate. However, we show that the critical velocity remains approximately constant within a considerable range of temperatures, contrary to expectation, and the thermal cloud has a stabilizing effect.

DOI: [10.1103/PhysRevA.104.033323](https://doi.org/10.1103/PhysRevA.104.033323)

I. INTRODUCTION

Ultracold atomic circuits have been realized in toroidal condensates with a tunable weak link [1–4]. Annular superfluids with a weak barrier inside can be used as nonlinear interferometers and are suitable for high-precision quantum devices or sensitive rotation sensors [5–8] and hence are practical in metrology [9].

Ring-shaped Bose-Einstein condensates in annular traps have been investigated both experimentally and theoretically [1–3,10–23]. In order to use such geometry for rotational sensors, however, the condensate needs to be stirred, and the decay of the persistent current via phase slips has to be controlled accurately [24–26]. As the rotation rate, Ω , increases from zero up to a few hertz, it may reach a threshold, Ω_{crit} , above which vortices enter into the bulk of the condensate. Ramanathan *et al.* [2] have already reported measurements of Ω_{crit} in a superfluid ring by observing the decay of a persistent current flowing past a stationary barrier.

Early experiments used simply connected condensates; the perturbing potential moved through the condensate [27–32] or used a phase imprinting technique [33,34], or the entire trap was rotated [35–37] to create vortices or dark solitons. Condensates in annular setups, however, represent a different topology, and the effect of geometry can be investigated more directly [38,39]. Furthermore, with the introduction of a weak link this setup provides a platform for creating sensors similar to the RF-superconducting quantum interference device (SQUID).

In atomtronics, a ring condensate is a central atomic circuit element; however, in practical applications one aims to control the thermal behavior of a sensor to achieve higher precision or less measurement uncertainty. Due to its practical importance,

here we investigate the thermal dependence of the critical angular frequency, Ω_{crit} , in a ring-shaped Bose-Einstein condensate (see inset of Fig. 1). In Ref. [40] we demonstrated that an effective one-dimensional model is sufficiently accurate to estimate Ω_{crit} , hence we use this model in the current study. For traps confining both condensate and thermal cloud two competitive phenomena, the depletion of the condensate and the effective potential due to the thermal cloud, keep the critical rotation speed almost unchanged for a considerable range of temperatures. This stability favors the further development of atomtronic devices based on annular setup.

II. THE GOVERNING EQUATION

At sufficiently low temperature a homogeneous, noninteracting, three-dimensional boson system undergoes a phase transition [41] and forms a Bose-Einstein condensate (BEC). At zero temperature the single-particle Schrödinger equation provides an adequate description. However, if weak and point-like interaction is considered, then a term proportional to the density must be included, and, in the mean-field approximation, one arrives at the Gross-Pitaevskii equation [11]

$$i\hbar \frac{\partial \Psi}{\partial t} = \left[-\frac{\hbar^2}{2m} \nabla^2 + V + \frac{4\pi \hbar^2 (N-1) a_s}{m} |\Psi|^2 \right] \Psi.$$

Above \hbar is the reduced Planck constant, m and a_s are the mass and s -wave scattering length of the particle species, respectively, while V is an external trap, and N is the number of particles.

In the following we focus on how thermal effects modify the dynamics of the condensate stirred by a potential barrier in an annular trap rotating at a rate of Ω . Transforming the equation of motion to a rotating reference frame introduces a new term, $-\Omega L_z$, where $L_z = -i\hbar[r \times \nabla]_z$. In order to render the new equation of motion dimensionless a length and timescale, a_0 and $\omega^{-1} = (\hbar/m a_0^2)^{-1}$, are introduced, and the variables are transformed as $t \mapsto t/\omega$, $\mathbf{x} \mapsto \mathbf{x} a_0$, $\Psi \mapsto \Psi a_0^{-3/2}$, $\Omega \mapsto \Omega \omega$, and $V \mapsto \hbar \omega V$. Keeping the original denotations, the

*ehsan.arabahmadi@postgrad.otago.ac.nz

†daniel.schumayer@otago.ac.nz

‡edwards@georgiasouthern.edu

§david.hutchinson@otago.ac.nz

dimensionless Gross-Pitaevskii equation reads as

$$i\frac{\partial\Psi}{\partial t} = \left[-\frac{1}{2}\nabla^2 + V + u_0N|\Psi|^2 - \Omega L_z\right]\Psi, \quad (1)$$

where $u_0 = 4\pi a_s/a_0$ and $(N-1)$ in the self-interaction term is replaced by N . For sodium atoms the parameters are $m = 3.8 \times 10^{-26}$ kg, and $a_s = 2.75$ nm [42–44]. For units we have chosen $a_0 = 10$ μm and $\omega \cong 2\pi \times 4.4$ rads $^{-1}$, with total number of atoms being $N = 2.9 \times 10^5$ corresponding to $u_0N \cong 1000$. These values are similar to the experimental value in Refs. [24,45,46].

III. REDUCED MODELS

Equation (1) can be reduced to a two-dimensional equation by assuming that the wave function can be factorized, $\Psi(x, y, z, t) = \psi(x, y, t)\psi_0(z)$, and in the z direction the condensate in its ground state, ψ_0 , of the trapping harmonic potential with a stationary barrier included. Integrating Eq. (1) with respect to z leads to [47]

$$i\frac{\partial\psi}{\partial t} = \left[-\frac{1}{2}\nabla^2 + U + \beta|\psi|^2 - \Omega L_z\right]\psi.$$

The condensate and the thermal cloud of atoms are trapped in the ring-shaped potential and then stirred by a potential barrier. The potential is the sum of these two terms: $U = U_{\text{trap}} + U_{\text{barrier}}$. The rotating barrier expels some of the atoms from a narrow arc in the trap, thereby creating a weak link between the condensate on the two sides of the barrier. The extent of this expulsion plays an important role in the following.

The annular trap is defined as

$$U_{\text{trap}}(r) = \frac{u_t}{2} \left[\tanh\left(\frac{R_1 - r}{b}\right) + \tanh\left(\frac{r - R_2}{b}\right) + 2 \right]$$

in which u_t is the depth of the potential trap and is taken to be large enough so that both the condensate and the thermal cloud are trapped within the annulus. The radii of the inner and the outer edge of the trap are $R_1 = 20$ μm and $R_2 = 30$ μm . These parameter values correspond to a critical temperature of ≈ 1020 nK. The parameter b controls the sharpness of potential edges and is chosen to be $b = 0.1$ μm . The stirrer can be created in an analogous manner, but in the angular variable, θ ,

$$U_{\text{barrier}}(\theta, t) = \frac{u_b}{2} \left[2 + \tanh\left(\frac{1}{b}\left[\theta - \theta_0(t) + \frac{\Delta\theta}{2}\right]\right) - \tanh\left(\frac{1}{b}\left[\theta - \theta_0(t) - \frac{\Delta\theta}{2}\right]\right) \right],$$

where u_b is height of the stirrer. The extra terms, compared to U_{trap} are the azimuthal width of the barrier, $\Delta\theta$, and the instantaneous center of the barrier, $\theta_0(t)$. The latter depends on time, and, for example, using $\theta_0(t) \propto t$ would simulate barrier rotating in a uniform manner. We change $\Delta\theta$, and $\theta_0(t)$ to study their effect on the dynamics of the condensate and the noncondensate cloud.

The two-dimensional problem can be simplified even further by neglecting any appreciable dynamics in the radial direction and considering the azimuthal angle θ or

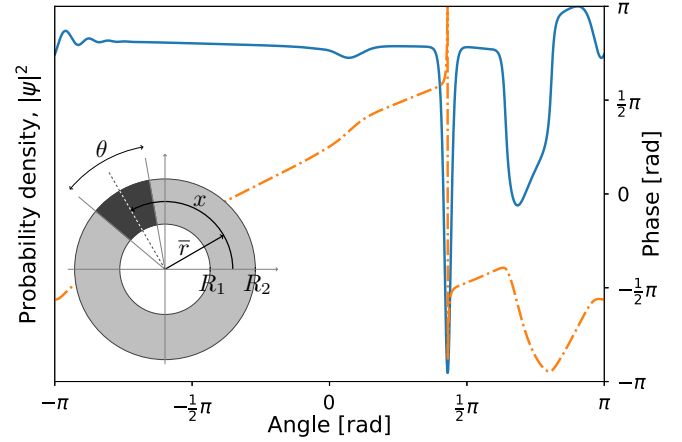


FIG. 1. Appearance of a phase slip (dashed line) through a dark soliton (solid line) for barrier height $u_b = 20$ and angular width of $\Delta\theta = \pi/6$. The snapshot is taken at $t = 3.59$ units after starting from rest with acceleration $\ddot{\theta} = 0.04$. (Inset) Overview of the ring-shaped confining trap (gray) with a barrier (dark gray) covering the entire channel width.

the corresponding arc-length x , along an effective radius \bar{r} , to be the only degree of freedom; i.e., the wave-function is further factorized as $\psi(r, \theta, t) = \Theta(x, t)R(r)$. Here $R(r)$ is calculated from the angular average of the ground-state density profile: $R^2(r) = \int |\psi_{\text{gs}}(r, \theta)|^2 r d\theta$. The effective one-dimensional Gross-Pitaevskii equation then becomes

$$i\frac{\partial\Theta}{\partial t} = H\Theta = \left[-\frac{1}{2}\frac{\partial^2}{\partial x^2} + U_{\text{barrier}} + \beta'|\Theta|^2 + i\bar{r}\Omega\frac{\partial}{\partial x}\right]\Theta, \quad (2)$$

augmented with periodic boundary condition for Θ . Furthermore, $\beta' = u'_0N$, where \bar{r} and u'_0 are

$$\bar{r} = \int r |R(r)|^2 dr \quad \text{and} \quad u'_0 = u_0 \int |R(r)|^4 dr.$$

In the two-dimensional problem the values $u_b = 4.3$ nK, $\Delta\theta = \pi/6$ were used, which translate to $\bar{r} \cong 25.3$ μm , and $\beta' \cong 963$. These numerical values were used in the effective one-dimensional description. Comparing the predictions of the one- and two-dimensional descriptions we found $\Omega_{\text{crit}}^{\text{1D}} = 1.21$ and $\Omega_{\text{crit}}^{\text{2D}} = 1.23$.

A phase slip occurs in this one-dimensional model by the creation of a dark soliton. In Fig. 1 one can see the process of phase slip through creation of solitons in the one-dimensional model.

In order to calculate the critical rotation speed of the barrier accurately, we calculate the ground-state solution in a corotating frame with the barrier present, and then sweep the rotation speed to see at what point the ground-state solution becomes unstable and changes to a solution with a 2π phase jump.

IV. THERMAL EFFECTS ON Ω_{crit}

Apart from the idealized case of noninteracting boson system at absolute zero temperature, some atoms occupy excited states and form a cloud. For an interacting system such a cloud is always present, even at zero temperature. Let us investigate the effect of this thermal cloud on Ω_{crit} by calculating the

excitations around a stationary solution of Eq. (2): $\Theta = \Theta_0 + z$. Substituting Θ and neglecting second-order terms in z we obtain

$$i \frac{dz}{dt} = Lz + Mz^* \quad (3)$$

with $L = -\frac{1}{2} \frac{\partial^2}{\partial x^2} + U_{\text{barrier}} + 2\beta'|\Theta_0|^2 - \Omega L_z - \mu$ and $M = \beta\Theta_0^2$. We also expand z in eigenmodes, u_k and v_k , considering both positive and negative frequencies

$$z = \sum_k u_k e^{-i\omega_k t} + v_k^* e^{i\omega_k t}.$$

Substituting this expansion into Eq. (3) one obtains the Bogoliubov–de Gennes (BdG) equations in the rotating frame:

$$\begin{pmatrix} L & M \\ -M^* & -L^* \end{pmatrix} \begin{pmatrix} u_k \\ v_k \end{pmatrix} = \omega_k \begin{pmatrix} u_k \\ v_k \end{pmatrix}. \quad (4)$$

If ω_k is real, then the stationary solution is stable, while the appearance of a complex frequency is a sign of instability. In this one-dimensional model the lowest frequency approaches zero as $\Omega \rightarrow \Omega_{\text{crit}}$ [40].

As the temperature increases more and more atoms can occupy higher energy states, hence the number of atoms in the thermal cloud increases, and thus the condensate is depleted more and more. Since Ω_{crit} is proportional to the condensate density, we expect Ω_{crit} to decrease with increasing temperature. However, contrary to our expectation, the effective potential, created by the thermal cloud, prevents the immediate reduction of Ω_{crit} and compensates for the depletion. The thermal cloud has a stabilizing effect maintaining the critical speed more or less constant in the temperature range examined. This conclusion is supported by the numerical simulation relying on the dimensionless Hartree-Fock-Bogoliubov approach augmented with the Popov approximation in rotating frame

$$\left[-\frac{1}{2} \frac{\partial^2}{\partial x^2} + U_{\text{barr}} + 2u'_0 \tilde{n}(x) + \beta'' |\Theta|^2 - \Omega L_z - \mu \right] \Theta = 0, \quad (5)$$

where β'' is the same as β' in Eq. (2) except the total number of atoms N is replaced with the number of condensate atoms, N_c . Furthermore, $\tilde{n}(x)$ is the density of the thermal cloud

$$\tilde{n}(x) = \sum_{k>0} [(1 + \bar{n}_k) |v_k(x)|^2 + \bar{n}_k |u_k(x)|^2], \quad (6)$$

where \bar{n}_k is the occupation number of the k th excitation mode with positive frequency, ω_k , and is given by the Bose-Einstein distribution. The number of atoms in the thermal cloud is

$$N_{\text{th}}(T) = \int \tilde{n}(x) dx,$$

while in the condensate $N_c(T) = N - N_{\text{th}}(T)$.

In order to find the critical speed of the barrier we start with $\Omega \ll \Omega_{\text{crit}}$ and solve Eq. (5) self-consistently for a stable ground-state solution. First, we obtain the ground-state solution Θ_0 of Eq. (2). Next the frequency eigenvalues and eigenfunctions are calculated from the BdG equation (4) from which $\tilde{n}(x)$ can be determined via Eq. (6). These quantities in hand, we are in a position to calculate the

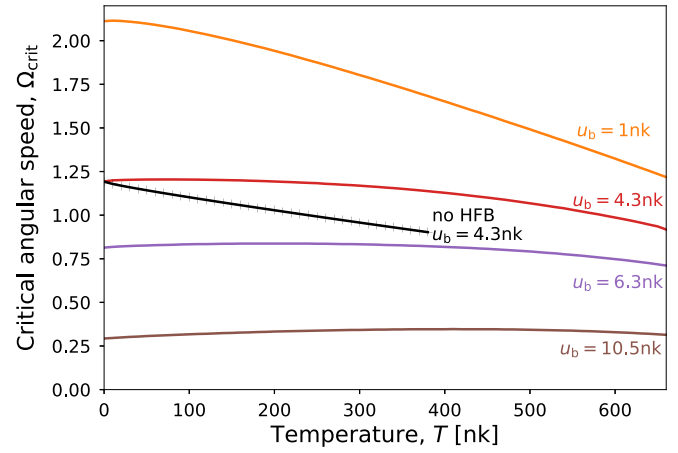


FIG. 2. Thermal behavior of the critical rotation speed of the barrier as a function of temperature. The four barrier heights, u_b , are given in temperature equivalent unit. The colored lines use the HFB-Popov approximation, while the black line assumes only depletion of the atoms in the condensate.

updated ground-state wave function Θ_0 via the Hartree-Fock-Bogoliubov-Popov approximation (5). After updating β'' , and $V_{\text{eff}} = U_{\text{barrier}} + 2u'_0 \tilde{n}(x)$, we replace β' and U_{barrier} with them in the definition of L , respectively, and solve Eq. (4) to obtain the new β'' and $\tilde{n}(x)$. We keep doing this iterative procedure until Θ_0 converges. We gradually increase Ω until we reach the critical value, Ω_{crit} , for which convergence cannot be achieved anymore. At Ω_{crit} the condensate wave function develops a 2π phase jump and a topologically different solution, a dark soliton, becomes the lowest energy solution. We might expect that the dominant effect of the temperature is to deplete the condensate, and this reduction in N_c decreases the nonlinear coupling, β , and hence Ω_{crit} decreases as well. Our calculations, however, show that the thermal cloud creates an effective potential, $V_{\text{eff}} = U_{\text{barrier}} + 2u'_0 \tilde{n}(x)$, and its distribution is such that it compensates for the depletion of the condensate for a wide range of temperatures.

In Fig. 2, Ω_{crit} is plotted as a function of temperature for five different barrier heights, u_b , and for a case where the Hartree-Fock-Bogoliubov approximation is not employed. One may notice neglecting the effects of the thermal cloud leads to a monotonically decreasing critical angular speed (black), while the other curves seem to be concave from below, even at a low barrier height. However, as u_b decreases (cf. top curve for the lowest u_b), and consequently the effect of thermal cloud is reduced, Ω_{crit} is flat only very close to the absolute zero and drops nearly at a similar rate as the “no HFB” curve. Earlier studies of cylindrically trapped condensates [48,49], following similar theoretical models, also support the conclusion that a rotating condensate can be stable even at nonzero temperatures

It is clear that the effective potential of the thermal cloud plays an important role even at zero temperature. To clarify its effect, one can see a plot of the potential barrier and the effective potential produced by the thermal cloud in Fig. 3 for $\Omega = 0.91 < \Omega_{\text{crit}}$, and $T = 100$ nK. It is clear that the effective potential is weaker in the barrier region as the density of the thermal atoms are mostly expelled from that region; however, the thermal cloud potential raises the level of the

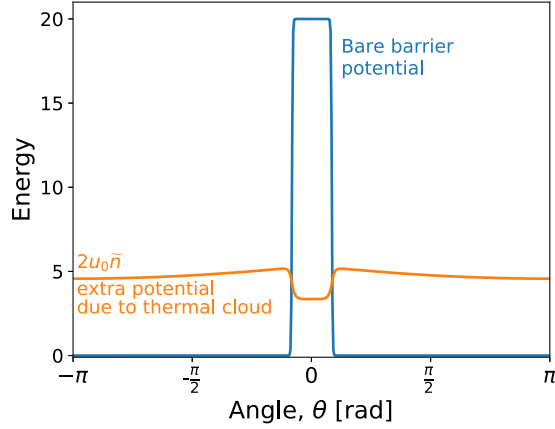


FIG. 3. The bare barrier potential and the effective potential created by the thermal cloud are depicted as a function of the central angle, θ . The sum of these two potentials form V_{eff} , which has a barrier with an effective height of $\cong 18$ instead of 20 units as in the bare potential. Hence the thermal cloud effectively reduced the barrier height.

total potential everywhere, but less in the barrier region, and its net result is reducing the barrier height.

We have shown [40] that $\Omega_{\text{crit}} \propto \beta'$ and $\Omega_{\text{crit}} \propto 1/u_b$. Hence, the result of this factor is to increase the critical velocity. On the other hand, reducing the number of atoms in the BEC by increasing temperature would tend to lower it. These two competing factors cancel out each other in some range of temperatures and causes the critical velocity to remain stable against variation of temperature. To compare the influence scale of these two factors, we can obtain the change in β' and the final barrier height V_{eff} at each temperature at a rotation frequency that is not very far from the critical velocity. We are aware of the fact that rotation changes the BdG spectrum, and consequently the change in the condensate number, and the effective barrier height. But we investigate what happens in a region that is not far from the critical velocity to obtain a qualitative explanation of the effect of these two factors.

In Ref. [40] we have given an implicit expression for Ω_{crit} in terms of the system parameters, e.g., the interaction strength β' and the effective barrier height, and we use that expression to evaluate the total change:

$$\Delta\Omega_{\text{crit}} = \left(\frac{\partial\Omega_{\text{crit}}}{\partial\beta'} \right)_{V_{\text{eff}}} \Delta\beta'(T) + \left(\frac{\partial\Omega_{\text{crit}}}{\partial V_{\text{eff}}} \right)_{\beta'} \Delta V_{\text{eff}}(T). \quad (7)$$

Both terms depend on temperature, and both $\Delta\beta'$ and ΔV_{eff} are negative for a barrier of height $u_b = 20$ and width

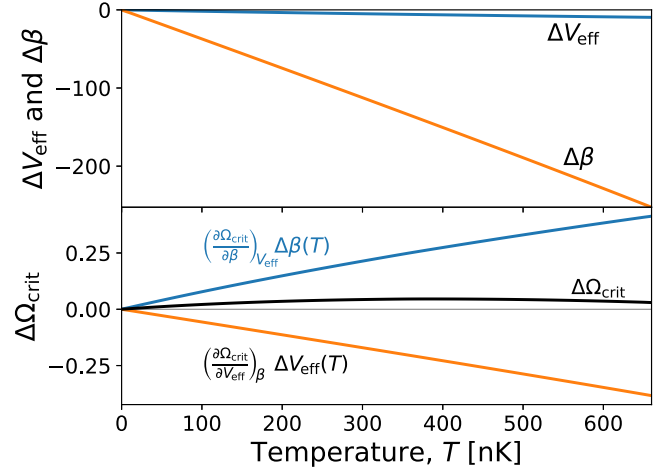


FIG. 4. (Top panel) Changes in the effective barrier height and the effective β' as a function of temperature. (Bottom panel) Variation of the critical frequency to the linear order of $\Delta\beta'(T)$, and $\Delta V_{\text{eff}}(T)$. They are calculated using our information about the thermal changes in β' , and V_b at a rotation close to the critical value ($\Omega = 0.91$).

$\Delta\theta = \frac{1}{6}\pi$ and at the rotation frequency $\Omega = 0.91$. In Fig. 4 it is apparent that their scale of variation is quite different. However, the sensitivity of the critical velocity to the barrier height, $\partial\Omega_{\text{crit}}/\partial V_{\text{eff}}$, is stronger than that to β' , and their signs are opposite. In the bottom panel of Fig. 4, we have plotted the first and second terms of Eq. (7) and their sum. It is apparent that the additive terms in Eq. (7) have opposite signs and nearly cancel each other; thus $\Delta\Omega_{\text{crit}}$ barely varies within the given temperature range.

V. CONCLUSION

We have studied the effect of thermal cloud on the critical angular speed of a rotating barrier at a wide range of temperature. We observed that the critical angular speed is quite stable with respect to temperature changes for strong enough barriers confining both the condensate and the thermal cloud. The results are inconsistent with the intuitive expectation that Ω_{crit} should decrease as particles leave the condensate thereby reducing the condensate density and consequently reducing the effect of the nonlinear term as well. This stability is the result of the reduction of the effective potential barrier height, caused by the thermal cloud, and it can compensate the effect of reduction of the condensate number.

- [1] C. Ryu, M. F. Andersen, P. Cladé, V. Natarajan, K. Helmerson, and W. D. Phillips, *Phys. Rev. Lett.* **99**, 260401 (2007).
- [2] A. Ramanathan, K. C. Wright, S. R. Muniz, M. Zelan, W. T. Hill, C. J. Lobb, K. Helmerson, W. D. Phillips, and G. K. Campbell, *Phys. Rev. Lett.* **106**, 130401 (2011).
- [3] K. C. Wright, R. B. Blakestad, C. J. Lobb, W. D. Phillips, and G. K. Campbell, *Phys. Rev. Lett.* **110**, 025302 (2013).

- [4] F. Jendrzejewski, S. Eckel, N. Murray, C. Lanier, M. Edwards, C. J. Lobb, and G. K. Campbell, *Phys. Rev. Lett.* **113**, 045305 (2014).
- [5] T. L. Gustavson, P. Bouyer, and M. A. Kasevich, *Phys. Rev. Lett.* **78**, 2046 (1997).
- [6] M. Edwards, *Nat. Phys.* **9**, 68 (2013).
- [7] C. Ryu, P. W. Blackburn, A. A. Blinova, and M. G. Boshier, *Phys. Rev. Lett.* **111**, 205301 (2013).

- [8] S. Ragole and J. M. Taylor, *Phys. Rev. Lett.* **117**, 203002 (2016).
- [9] J. Clarke, *The SQUID Handbook* (Wiley-VCH, Weinheim, 2003).
- [10] K. Kasamatsu, M. Tsubota, and M. Ueda, *Phys. Rev. A* **66**, 053606 (2002).
- [11] A. J. Leggett, *Quantum Liquids* (Oxford University Press, Oxford, 2006).
- [12] M. Benakli, S. Raghavan, A. Smerzi, S. Fantoni, and S. R. Shenoy, *Europhys. Lett.* **46**, 275 (1999).
- [13] J. Brand and W. P. Reinhardt, *J. Phys. B: At., Mol. Opt. Phys.* **34**, L113 (2001).
- [14] A. Das, J. Sabbatini, and W. H. Zurek, *Sci. Rep.* **2**, 352 (2012).
- [15] J.-P. Martikainen, K.-A. Suominen, L. Santos, T. Schulte, and A. Sanpera, *Phys. Rev. A* **64**, 063602 (2001).
- [16] J. D. Pritchard, A. N. Dinkelaker, A. S. Arnold, P. F. Griffin, and E. Riis, *New J. Phys.* **14**, 103047 (2012).
- [17] M. Modugno, C. Tozzo, and F. Dalfovo, *Phys. Rev. A* **74**, 061601(R) (2006).
- [18] P. F. Griffin, E. Riis, and A. S. Arnold, *Phys. Rev. A* **77**, 051402(R) (2008).
- [19] S. Beattie, S. Moulder, R. J. Fletcher, and Z. Hadzibabic, *Phys. Rev. Lett.* **110**, 025301 (2013).
- [20] A. I. Yakimenko, K. O. Isaieva, S. I. Vilchinskii, and M. Weyrauch, *Phys. Rev. A* **88**, 051602(R) (2013).
- [21] P. Mason and N. G. Berloff, *Phys. Rev. A* **79**, 043620 (2009).
- [22] K. C. Wright, R. B. Blakestad, C. J. Lobb, W. D. Phillips, and G. K. Campbell, *Phys. Rev. A* **88**, 063633 (2013).
- [23] Y. Guo, R. Dubessy, M. d. G. de Herve, A. Kumar, T. Badr, A. Perrin, L. Longchambon, and H. Perrin, *Phys. Rev. Lett.* **124**, 025301 (2020).
- [24] S. Moulder, S. Beattie, R. P. Smith, N. Tammuz, and Z. Hadzibabic, *Phys. Rev. A* **86**, 013629 (2012).
- [25] F. Piazza, L. A. Collins, and A. Smerzi, *Phys. Rev. A* **80**, 021601(R) (2009).
- [26] F. Piazza, L. A. Collins, and A. Smerzi, *J. Phys. B: At., Mol. Opt. Phys.* **46**, 095302 (2013).
- [27] C. Raman, M. Köhl, R. Onofrio, D. S. Durfee, C. E. Kuklewicz, Z. Hadzibabic, and W. Ketterle, *Phys. Rev. Lett.* **83**, 2502 (1999).
- [28] R. Onofrio, C. Raman, J. M. Vogels, J. R. Abo-Shaeer, A. P. Chikkatur, and W. Ketterle, *Phys. Rev. Lett.* **85**, 2228 (2000).
- [29] C. Raman, R. Onofrio, J. M. Vogels, J. R. Abo-Shaeer, and W. Ketterle, *J. Low Temp. Phys.* **122**, 99 (2001).
- [30] S. Inouye, S. Gupta, T. Rosenband, A. P. Chikkatur, A. Görlitz, T. L. Gustavson, A. E. Leanhardt, D. E. Pritchard, and W. Ketterle, *Phys. Rev. Lett.* **87**, 080402 (2001).
- [31] P. Engels and C. Atherton, *Phys. Rev. Lett.* **99**, 160405 (2007).
- [32] T. W. Neely, E. C. Samson, A. S. Bradley, M. J. Davis, and B. P. Anderson, *Phys. Rev. Lett.* **104**, 160401 (2010).
- [33] S. Burger, K. Bongs, S. Dettmer, W. Ertmer, K. Sengstock, A. Sanpera, G. V. Shlyapnikov, and M. Lewenstein, *Phys. Rev. Lett.* **83**, 5198 (1999).
- [34] J. Denschlag, J. E. Simsarian, D. L. Feder, C. W. Clark, L. A. Collins, J. Cubizolles, L. Deng, E. W. Hagley, K. Helmerson, W. P. Reinhardt, S. L. Rolston, B. I. Schneider, and W. D. Phillips, *Science* **287**, 97 (2000).
- [35] K. W. Madison, F. Chevy, W. Wohlleben, and J. Dalibard, *Phys. Rev. Lett.* **84**, 806 (2000).
- [36] P. C. Haljan, I. Coddington, P. Engels, and E. A. Cornell, *Phys. Rev. Lett.* **87**, 210403 (2001).
- [37] J. R. Abo-Shaeer, C. Raman, J. M. Vogels, and W. Ketterle, *Science* **292**, 476 (2001).
- [38] B. E. Sherlock, M. Gildemeister, E. Owen, E. Nugent, and C. J. Foot, *Phys. Rev. A* **83**, 043408 (2011).
- [39] G. E. Marti, R. Olf, and D. M. Stamper-Kurn, *Phys. Rev. A* **91**, 013602 (2015).
- [40] E. Arabahmadi, D. Schumayer, and D. A. W. Hutchinson, *Phys. Rev. A* **103**, 043319 (2021).
- [41] R. K. Pathria, *Statistical Mechanics*, International Series of Monographs in Natural Philosophy, Vol. 45 (Pergamon Press, Oxford, New York, 1972).
- [42] R. Côté and A. Dalgarno, *Phys. Rev. A* **50**, 4827 (1994).
- [43] E. Tiesinga and C. J. Williams, *J. Res. Natl. Inst. Stand. Technol.* **101**, 505 (1996).
- [44] K. B. Davis, M.-O. Mewes, M. R. Andrews, N. J. van Druten, D. S. Durfee, D. M. Kurn, and W. Ketterle, *Phys. Rev. Lett.* **75**, 3969 (1995).
- [45] A. Kumar, N. Anderson, W. D. Phillips, S. Eckel, G. K. Campbell, and S. Stringari, *New J. Phys.* **18**, 025001 (2016).
- [46] E. C. Samson, K. E. Wilson, Z. L. Newman, and B. P. Anderson, *Phys. Rev. A* **93**, 023603 (2016).
- [47] X. Antoine and R. Duboscq, *Comput. Phys. Commun.* **185**, 2969 (2014).
- [48] T. Isoshima and K. Machida, *Phys. Rev. A* **59**, 2203 (1999).
- [49] S. M. M. Virtanen, T. P. Simula, and M. M. Salomaa, *Phys. Rev. Lett.* **86**, 2704 (2001).